International Journal of Thermofluid Science and Technology (2019)
Volume 6, Issue 1, Paper No. 19060102
https://doi.org/10.36963/IJTST.19060102
Research Article

Finite strip method applied to steady heat conduction and thermal radiation in a planar slab: absorbing −emitting gray material and parallel diffuse surfaces

Severno P. C. Marques[1], Antonio Campo[2]

[1]*Center of Engineering Technology, Federal University of Alagoas, Maceio, AL, 57072-870, Brazil*
[2]*Department of Mechanical Engineering, The University of Vermont, Burlington, VT 05405, USA*

Received: 5 June 2019; Received in revised form: 28 August 2019; Accepted: 10 October 2019;
Published online: 10 November 2019

Abstract

This paper addresses a new finite strip method for the analysis of simultaneous heat conduction and thermal radiation in a planar slab with diffuse surfaces and filled with an absorbing and emitting material considered as a gray medium. The gray material is discretized into a finite number of strips where the temperature is approximated with quadratic expansions in local coordinates whose coefficients are unknowns inside each strip. The finite strip method consists in a set of discrete equations corresponding to energy balance equations united to the compatibility conditions of both temperature and heat flux between consecutive strips. The gray material is articulated with different combinations of thermal and optical properties. Numerical results for the temperature fields and the conductive, radiative and total heat fluxes are presented in graphical and tabular forms and they compared favorably with equivalent results employing standard calculation techniques. The three main features attributable to the finite strip method are simplicity, quick calculation, good convergence and quality results.

Keywords: simultaneous heat conduction and thermal radiation, planar slab, diffuse surfaces, absorbing-emitting gray material, new finite strip methodology.

1. Introduction

The combination of heat conduction and thermal radiation mechanisms is normally encountered in semitransparent materials as cited in the textbooks by Howell et al. (2011) and Modest (2013). Practical engineering applications of semitransparent solids, such as industrial

Corresponding email: campanto@yahoo.com (Antonio Campo)

furnaces, glass manufacturing, fiber and foam insulations, high performance windows, solar collectors have been reported in publications by Viskanta and Anderson (1975) and Campo et al. (1986,1987).

Nomenclature

d	thickness of a typical finite strip	κ	optical coordinate
D	thickness of the planar slab	μ	cosine of radiation direction
E_n	exponential integral function, eq. (5)	Θ	non-dimensional temperature, $\Theta = T/T_1$
i	total intensity	σ	Stefan-Boltzmann constant
K	extinction coefficient	ψ	equation in the system of nonlinear algebraic equations
K_D	optical thickness	ζ	non-dimensional total heat flux, $\zeta = q/(\sigma T_{ref}^4)$
L	total number of finite strips		
N	conduction-radiation parameter	*Subscripts*	
q	heat flux	b	blackbody
T	temperature and temperature coefficient	c	conduction
dT/dx	temperature gradient	r	radiation
x	Cartesian coordinate	t	total = conduction plus radiation
$\overline{x}$	local coordinate at the mid-plane of a strip	n	order of the exponential integral function E_n
		i, j, γ	indices
Greek symbols		m	iterative step
α	typical finite strip		
β_c	thermal conductivity	*Superscripts*	
$\delta_{\alpha\gamma}$	Kronecker delta function	$+$	refers to forward direction
ε	surface emissivity	$-$	refers to backward direction
η	refractive index	$*$	optical coordinate for integration

Several theoretical and numerical studies exist for the prediction of the total heat transfer by simultaneous conduction and radiation in gray materials; that is materials with extinction coefficient independent of wavelength. As noted by Mishra et al. (2006), theoretical models for the quantification of radiation heat transfer have been recognized as computationally intensive and time consuming. These features are attributed to the difficulty and high processing cost involving the radiation mechanism, which are due to the integro-differential nature of the governing energy equations (Howell et al. (2011) and Modest (2013). However, reasonable efforts have been directed in the past to reduce the processing time by developing new models and enhancing the computational procedures of the existing models. Representative publications on these efforts are those by Mishra et al. (2004), Anteby et al. (2000), Ratzell III and Howell

(1982). A pioneering theoretical formulation for radiation heat transfer in a planar slab was developed by Viskanta and Grosh (1962a). These authors generated a rigorous solution for the case of one-dimensional gray medium by way of a complex procedure that transforms the integro-differential energy equation into a nonlinear integral energy equation. The nonlinear integral equation was solved by an iterative procedure. The authors also extended their formulation to investigate the effects of boundary emissivities on radiation heat transfer in a gray medium (Viskanta and Grosh, 1962b). More recently, the discrete transfer method (Shah, 1979) and the collapsed dimension method (Mishra, 1997) have been implemented to address the same problem. Afterwards, a comparative study between the two methods was carried out in Talukdar and Mishra (2002). The emerging results are in very good agreement with those published by Viskanta and Grosh (1962a,b). However, an inevitable drawback was that the number of iterations required for sub-problems dominated by radiation is very large. According to Talukdar and Mishra (2002), for sub-problems dictated by conduction-radiation parameters N smaller or equal to 0.01 an under relaxation technique is mandatory to attain satisfactory convergence.

For a particular case of transparent materials, Dai and Fang (2014) used the thermal response factor method developed by Mitalas (1968) to estimate the heat transmission in bodies. In fact, the peculiarity of this work is that the absorbed solar radiation was treated as an internal source term in the descriptive energy equation.

The objective of the present work revolves around the application of a new finite strip method for the heat transfer analysis by simultaneous heat conduction and thermal radiation in an absorbing and emitting gray material forming a planar slab. Further, convection heat transfer is ignored. The method in question consists of an iterative tangent nonlinear formulation in which the gray medium is discretized into a finite number of strips. Inside each finite strip, the temperature variation is approximated using quadratic expansions in local coordinates whose coefficients are the primary unknowns in the problem. The resulting discrete equations correspond to a collection of balance energy equations and compatibility conditions of temperature and heat flux between successive strips. Unquestionably, the main features inherent to the finite strip method are simplicity and quick convergence. For verification, the finite strip method is applied to a planar slab problem with different combinations of thermal and optical properties. Numerical results in terms of temperature fields as well as conductive, radiative and total heat fluxes are presented in graphical and tabulated forms. Besides, the relative importance of each heat transfer mode is elucidated. A detailed comparison of the numerical results with others obtained by well established theoretical models demonstrates a good balance between accuracy and the number of iterations needed for convergence.

2. Steady Conservation Equation of Energy

A planar slab of thickness D made from a homogeneous, isotropic material is sketched in Figure 1. The material filling the planar slab is assumed to be gray, absorbing, emitting and non-scattering. For simplicity, the material properties are considered independent of temperature. The bounding parallel surfaces 1 and 2 in the planar slab are idealized as opaque and diffuse and are

maintained at temperatures T_1 and T_2. It is envisioned that heat transfer in the planar slab occurs by simultaneous heat conduction and thermal radiation. In addition, to avoid convection heat transfer, the planar slab is situated in a perfect vacuum.

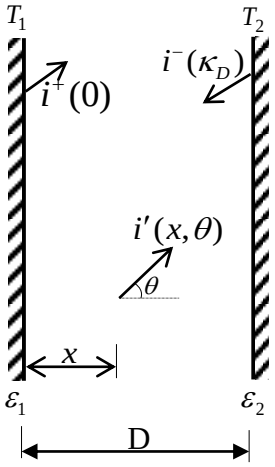

Fig.1 Planar slab with two diffuse boundary surfaces housing an absorbing-emitting gray material. The left and right boundary surfaces are kept at temperatures T_1 and T_2 respectively.

The one dimensional geometry is a good approximation for the energy transport in many physical situations, such as insulation, atmospheres and furnaces. Besides, the one dimensional geometry is also a building block for the preliminary analysis of more involved geometries dealing with two and three dimensions.

Under steady-state conditions, the total heat flux q_t through the planar slab is constant. Thereby, the total heat flux q_t is quantified by the additive relation

$$q_t = q_c(x) + q_r(x) \tag{1}$$

where $q_c(x)$ is the conductive heat flux and $q_r(x)$ is the radiative heat flux occurring at the point with coordinate x as illustrated in Figure 1. The conductive heat flux $q_c(x)$ is obtained from Fourier's law (Arpaci, 1966):

$$q_c(x) = -\beta_c \frac{dT}{dx} \tag{2}$$

where β_c is the thermal conductivity. Upon introducing the optical coordinate $\kappa = Kx$, where K is the material extinction coefficient, the radiative heat flux $q_r(x)$ as given by Howell et al. (2011) and Modest (2013) is:

$$q_r(\kappa) = 2\pi[i^+(0)E_3(\kappa) - i^-(\kappa_D)E_3(\kappa_D - \kappa) + \int_0^{\kappa} \eta^2 i_b'(\kappa^*)E_2(\kappa - \kappa^*)d\kappa^* - \int_{\kappa}^{\kappa_D} \eta^2 i_b'(\kappa^*)E_2(\kappa^* - \kappa)d\kappa^*] \tag{3}$$

In this equation, $i^+(0)$ and $i^-(\kappa_D)$ represent the forward and backward total intensities at the bounding surfaces 1 and 2, respectively, κ_D is the optical thickness and η is the refractive index of the gray material. Furthermore, $\mu = \cos\theta$, wherein θ is the angle between the radiation direction and the x-axis as indicated in Figure 1. The blackbody total intensity i_b' depends on the temperature T with the formula (Howell et al., 2011 and Modest, 2013).

$$i_b' = \frac{\sigma}{\pi} T^4 \tag{4}$$

where the Stefan-Boltzmann constant $\sigma = 5.67\times10^{-8}$ W/(m^{2}K^4). The quantities $E_2()$ and $E_3()$ in Eq. (3) emerge from the exponential integral function (Abramowitz and Stegun, 1965):

$$E_n(\xi) = \int_0^1 \mu^{n-2} e^{-\xi/\mu} d\mu \tag{5}$$

for $n = 2$ and $n = 3$.

The total intensities $i^+(0)$ and $i^-(\kappa_D)$ at the two bounding surfaces 1 and 2 can be evaluated by the pair of expressions

$$i^+(0) = \varepsilon_1 \eta^2 i_{b,1}' + 2(1-\varepsilon_1)\left[i^-(\kappa_D)E_3(\kappa_D) + \int_o^{\kappa_D} \eta^2 i_b'(\kappa^*)E_2(\kappa^*)d\kappa^* \right] \tag{6a}$$

and

$$i^-(\kappa_D) = \varepsilon_2 \eta^2 i_{b,2}' + 2(1-\varepsilon_2)\left[i^+(0)E_3(\kappa_D) + \int_o^{\kappa_D} \eta^2 i_b'(\kappa^*)E_2(\kappa_D - \kappa^*)d\kappa^* \right] \tag{6b}$$

where ε_1 and ε_2 denote the respective surface emissivity of bounding surfaces 1 and 2.

Within the platform of simultaneous conduction-radiation heat transfer, the governing conservation equation of energy is taken from Howell et al. (2011) and Modest (2013):

$$\nabla \cdot (\beta_c \nabla T - q_r) = 0 \tag{7}$$

Using Eqs. (2) and (3), allows us to write Eq. (7) in the form of a nonlinear integro-differential equation

$$\beta_c \frac{d^2T}{dx^2} + 2\pi K[i^+(0)E_2(\kappa) + i^-(\kappa_D)E_2(\kappa_D - \kappa) + \int_0^{\kappa} \eta^2 i_b'(\kappa^*)E_1(\kappa - \kappa^*)d\kappa^* + \int_{\kappa}^{\kappa_D} \eta^2 i_b'(\kappa^*)E_1(\kappa^* - \kappa)d\kappa^* - 2\eta^2 i_b'(\kappa)] = 0 \tag{8}$$

which is subject to the prescribed temperature boundary conditions

$$T(0) = T_1 \text{ and } T(D) = T_2 . \tag{9}$$

From a fundamental framework, the pair of Eqs. (8) and (9) constitutes a nonlinear and nonlocal problem. On one hand, the nonlinear part presents difficulties because the blackbody total intensity i_b' depends on the temperature field *T (x)*, which is not known a priori. On the other hand, the non-local part implies that the total heat flux q_t at a point *x* depends on both the temperature *T (x)* and the temperature gradient *dT/dx.*

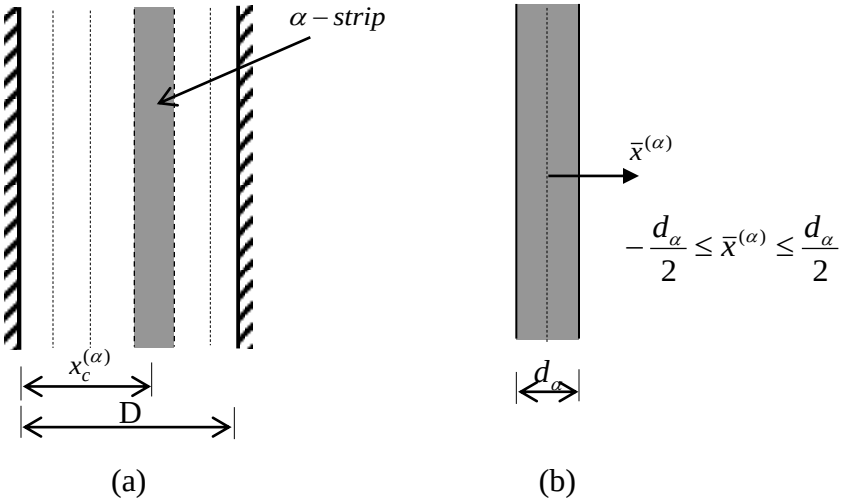

Fig.2 (a) Planar slab divided into *L* finite strips and (b) local coordinate system in a typical $\alpha-$strip shown in part (a).

3. Numerical Computational Procedure: The New Finite Strip Method

Owing that the central objective in the study is to produce manageable discrete equations, the planar slab is divided into a finite number of *L* strips, each with variable thickness d_α $(1 \le \alpha \le L)$ as shown in Figure 2. Accordingly, a local coordinate $\bar{x}^{(\alpha)}$ is assigned at the mid-plane of each strip, so that $-\frac{d_\alpha}{2} \le \bar{x}^{(\alpha)} \le \frac{d_\alpha}{2}$.

The temperature *T (x)* at each strip is approximated by means of a quadratic expansion in the corresponding local coordinate $\bar{x}$. Correspondingly, for a typical $\alpha-$strip, the temperature is given by the equation

$$T(\bar{x}) = T_o^{(\alpha)} + \bar{x} T_1^{(\alpha)} + \frac{1}{2}\left(3\bar{x}^2 - \frac{d_\alpha^2}{4}\right) T_2^{(\alpha)} \tag{10}$$

where $T_o^{(\alpha)}$, $T_1^{(\alpha)}$ and $T_2^{(\alpha)}$ are the unknown temperature coefficients. It can be shown that: a) $T_o^{(\alpha)}$ represents the mean temperature in the $\alpha-$strip and b) $\beta_c T_1^{(\alpha)}$ is the conduction heat flux at the mid-plane of the $\alpha-$strip. Using this approximate temperature field, the energy equation (8) specialized at the mid-plane $\bar{x}^{(\alpha)}=0$ of the $\alpha-$strip can be channeled through the following expression

$$\begin{aligned}\psi_\alpha &= 3\beta_c T_2^{(\alpha)} + 2\pi K[i^+(0)E_2(\kappa_c^{(\alpha)}) + i^-(\kappa_D)E_2(\kappa_D-\kappa_c^{(\alpha)})\\ &+ \eta^2\sum_{\gamma=1}^{\alpha-1}\int_{\kappa_1^{(\gamma)}}^{\kappa_2^{(\gamma)}} i_b'(\kappa^*)E_1(\kappa_c^{(\alpha)}-\kappa^*)d\kappa^* + \eta^2\int_{\kappa_1^{(\alpha)}}^{\kappa_2^{(\alpha)}} i_b'(\kappa^*)E_1(\left|\kappa_c^{(\alpha)}-\kappa^*\right|)d\kappa^*\\ &+\eta^2\sum_{\gamma=\alpha+1}^{L}\int_{\kappa_1^{(\gamma)}}^{\kappa_2^{(\gamma)}} i_b'(\kappa^*)E_1(\kappa^*-\kappa_c^{(\alpha)})d\kappa^* - 2\eta^2 i_b'(\kappa_c^{(\alpha)})] = 0\end{aligned} \tag{11}$$

where $\kappa_c^{(\alpha)}$ is the optical coordinate at the mid-plane of the strip. The partial derivatives of ψ_α with respect to the unknown temperature coefficients $T_o^{(\gamma)}$, $T_1^{(\gamma)}$ and $T_2^{(\gamma)}$ associated with the $\gamma-$strip are represented by the following system of integro-partial differential equations

$$\begin{aligned}\frac{\partial\psi_\alpha}{\partial T_o^{(\gamma)}} &= 2\pi K[\frac{\partial i^+(0)}{\partial T_o^{(\gamma)}}E_2(\kappa_c^{(\alpha)}) + \frac{\partial i^-(\kappa_D)}{\partial T_o^{(\gamma)}}E_2(\kappa_D-\kappa_c^{(\alpha)})\\ &+ \eta^2\int_{\kappa_1^{(\gamma)}}^{\kappa_2^{(\gamma)}}\frac{\partial i_b'(\kappa^*)}{\partial T}E_1(\left|\kappa_c^{(\alpha)}-\kappa^*\right|)d\kappa^* - 2\eta^2\delta_{\alpha\gamma}\frac{\partial i_b'(\kappa_c^{(\alpha)})}{\partial T}] = 0\end{aligned} \tag{12}$$

$$\begin{aligned}\frac{\partial\psi_\alpha}{\partial T_1^{(\gamma)}} &= 2\pi K[\frac{\partial i^+(0)}{\partial T_1^{(\gamma)}}E_2(\kappa_c^{(\alpha)}) + \frac{\partial i^-(\kappa_D)}{\partial T_1^{(\gamma)}}E_2(\kappa_D-\kappa_c^{(\alpha)})\\ &+ \eta^2\int_{\kappa_1^{(\gamma)}}^{\kappa_2^{(\gamma)}}\frac{\partial i_b'(\kappa^*)}{\partial T}\bar{x}^{(\gamma)}E_1(\left|\kappa_c^{(\alpha)}-\kappa^*\right|)d\kappa^* - 2\eta^2\delta_{\alpha\gamma}\frac{\partial i_b'(\kappa_c^{(\alpha)})}{\partial T}\bar{x}^{(\gamma)}] = 0\end{aligned} \tag{13}$$

$$\begin{aligned}\frac{\partial\psi_\alpha}{\partial T_2^{(\gamma)}} &= 3\beta_c\delta_{\alpha\gamma} + 2\pi K[\frac{\partial i^+(0)}{\partial T_2^{(\gamma)}}E_2(\kappa_c^{(\alpha)}) + \frac{\partial i^-(\kappa_D)}{\partial T_2^{(\gamma)}}E_2(\kappa_D-\kappa_c^{(\alpha)})\\ &+ \eta^2\int_{\kappa_1^{(\gamma)}}^{\kappa_2^{(\gamma)}}\frac{\partial i_b'(\kappa^*)}{\partial T}\frac{1}{2}(3\bar{x}^{(\gamma)2}-\frac{d_\gamma^2}{4})E_1(\left|\kappa_c^{(\alpha)}-\kappa^*\right|)d\kappa^* - \eta^2\delta_{\alpha\gamma}\frac{\partial i_b'(\kappa_c^{(\alpha)})}{\partial T}(3\bar{x}^{(\gamma)2}-\frac{d_\gamma^2}{4})] = 0\end{aligned} \tag{14}$$

where $\delta_{\alpha\gamma}$ stands for the Kronecker delta function.

Under the premises that the finite strips are thin, the blackbody total intensities i_b' along with their derivatives in Eqs. (12)-(14) can be approximately evaluated in terms of the mean temperature T_o in each strip. By way of this simplification, the exponential integral functions E_n

over the optical coordinate can be evaluated explicitly. The integrals can be treated with different quadrature schemes, such as Gaussian, Lobatto, Chebyshev, and Newton-Cotes (Press et al., 1986). The integrals in question are of the form

$$\int_a^b f(\mu)d\mu = \sum_{j=1}^{n} w_j f(\mu_j) \tag{15}$$

where w_j are the weight coefficients corresponding to the n discrete points μ_j. The differences between the various quadrature schemes lie in the values of w_j and μ_j. Consider $f(\mu)$ to be a polynomial of degree m, having $m+1$ coefficients. For Gaussian quadrature, which contains the $2n$ weights and points to be arbitrary, the maximum value of m for which the summation is exact is $m = 2n - 1$. In this work, the precise four-point Gaussian quadrature scheme (Press et al., 1986) was implemented.

Actually, the present model generates a system of L energy equations, wherein each equation is connected to a particular finite strip. It is important to add that the energy equations depend on the unknown temperature coefficients. As expected, additional equations have to be written to comply with the compatibility conditions of temperature and heat flux at the interfaces of adjacent finite strips. In equation form, these compatibility conditions are equivalent to:

a) The temperature compatibility at the interface between two adjacent strips is

$$T^{(\alpha-1)}\left(\overline{x} = \frac{d_{\alpha-1}}{2}\right) = T^{(\alpha)}\left(\overline{x} = -\frac{d_\alpha}{2}\right) \tag{16a}$$

$$T_o^{(\alpha-1)} + \frac{d_{\alpha-1}}{2}T_1^{(\alpha-1)} + \frac{d_{\alpha-1}^2}{4}T_2^{(\alpha-1)} = T_o^{(\alpha)} - \frac{d_\alpha}{2}T_1^{(\alpha)} + \frac{d_\alpha^2}{4}T_2^{(\alpha)} \tag{16b}$$

b) The conduction heat flux compatibility at the interface between two adjacent strips is

$$q_c^{(\alpha-1)}\left(\overline{x} = \frac{d_{\alpha-1}}{2}\right) = q_c^{(\alpha)}\left(\overline{x} = -\frac{d_\alpha}{2}\right) \tag{17a}$$

$$T_1^{(\alpha-1)} + \frac{3d_{\alpha-1}}{2}T_2^{(\alpha-1)} = T_1^{(\alpha)} - \frac{3d_\alpha}{2}T_2^{(\alpha)} \tag{17b}$$

Besides, the temperature boundary conditions at the bounding surfaces are

$$T_o^{(1)} - \frac{d_1}{2}T_1^{(1)} + \frac{d_1^2}{4}T_2^{(1)} = T_1 \tag{18a}$$

$$T_o^{(L)} + \frac{d_L}{2}T_1^{(L)} + \frac{d_L^2}{4}T_2^{(L)} = T_2 \tag{18b}$$

Overall, a nonlinear system of algebraic equations consisting of $3L$ equations and $3L$

unknown temperature coefficients is formed by Eqs. (11), (16), (17) and (18). In general, the nonlinear system of algebraic equations can be written compactly as follows

$$\psi_i(\vec{T}) = 0 \qquad (i = 1,2,\ldots..3L) \tag{19}$$

where $\vec{T}$ is the vector of temperature coefficients

$$\vec{T} = \left\{T_0^{(1)} T_1^{(1)} T_2^{(1)} T_0^{(2)} T_1^{(2)} T_2^{(2)} \ldots\ldots T_0^{(L)} T_1^{(L)} T_2^{(L)}\right\} \tag{20}$$

An iterative solution procedure is implemented to solve the above system of algebraic equations. Applying the Taylor's series expansion of ψ_i to the vector $\vec{T}_m$ corresponding to a certain iteration *m*, a linearization technique leads to the equation

$$\psi_i(\vec{T}_{m+1}) \approx \psi_i(\vec{T}_m) + \left(\frac{\partial \psi_i}{\partial \vec{T}}\right)_{\vec{T}-\vec{T}_m} \times \delta\vec{T}_m = 0 \tag{21}$$

After neglecting higher order terms. In this equation, $\left(\frac{\partial \psi_i}{\partial \vec{T}}\right)$ represents the Jacobian matrix of the function ψ_i and $\delta\vec{T}_m$ indicates the incremental vector of temperature coefficients defined by

$$\delta\vec{T}_m = \vec{T}_{m+1} - \vec{T}_m \tag{22}$$

Next, combining Eqs. (21) and (22), the unknown temperature coefficients T_{m+1} are obtained iteratively using the equation

$$\vec{T}_{m+1} = \vec{T}_m - \left(\frac{\partial \psi_i}{\partial \vec{T}}\right)^{-1}_{\vec{T}-\vec{T}_m} \times \psi_i(\vec{T}_m) = 0 \tag{23}$$

Here, the iterative process begins by guessing an initial temperature field in the gray material occupying the planar slab, which is associated with the limiting condition of heat conduction.

Convergence of the nonlinear system of algebraic equations in Eq. (19) is achieved when the Euclidean norm of the n-th increment of temperature normalized by the temperature is less than a pre-set tolerance. Then, the convergence criterion is given by the ratio

$$\frac{\|\delta\vec{T}_m\|}{|T_{max}|} \leq tolerance \tag{24}$$

where $\|\ \|$ represents the Euclidian norm and $|T_{\max}|$ signifies the absolute value of the larger temperature between T_1 and T_2. The pre-set tolerance is usually set at 10^{-3}. Excellent convergence patterns are obtained employing a relatively small number of iterations (normally, from two to six) in the algorithm.

4. Validation of the New Finite Strip Method

The conduction-radiation parameter is defined by $N = \beta_c K / 4\sigma T_{ref}^3$, where β_c is the thermal conductivity, K is the extinction coefficient and T_{ref} is a reference temperature. In this work, T_{ref} has been taken as the largest temperature at the bounding surfaces, i.e., either T_1 or T_2. For high values of the conduction-radiation parameter N, heat conduction is the dominant mechanism, whereas for small values of N, thermal radiation is the dominant mechanism.

For gray materials, the accuracy of the algorithm has to be demonstrated by comparing the computed results provided by the new finite strip method in terms of temperature and heat fluxes with comparable published results that are available in the heat transfer literature.

For the computational domain, uniform meshes with 100, 150 and 200 finite strips are constructed. The number of iterations required for convergence usually varied between n = 2 and 6, being the maximum value ($n = 6$) associated with the limiting case of pure radiation $N = 0$. An adequate tolerance with an error equal to 0.001 is imposed. As it can be seen in Figure 3, the non-dimensional temperature distributions are in excellent agreement with those published by Talukdar and Mishra (2002). It should be added that in the paper by these authors, the number of iterations required for gray materials having various conduction-radiation parameters $N = 0.1,\ 0.01,\ 0.001$ and 0.0001 amounts to 80, 120, 600 and 650, respectively. For those particular cases connected to very small conduction-radiation parameter, such as $N \le 0.01$ under relaxation was necessary.

5. Presentation and Discussion of the Numerical Results

Figure 3 displays the non-dimensional temperature distributions $\Theta = T/T_1$ varying with the relative distance x/D for the case of a gray material owing an optical thickness $\kappa_D = 1$, temperature ratio $T_2/T_1 = 0.5$ coupled with four conduction-radiation parameter N = 0, 0.01, 0.1 and 10 together with a high surface emissivity $\varepsilon = 1.0$. With the exception of a high N = 10, the three non-dimensional temperature distributions exhibit a characteristic S-shape. For limiting pure radiation with N = 0 and weak radiation with N = 0.01 the two non-dimensional temperature distributions coincided with those obtained by Talukdar and Mishra (2002). For limiting pure radiation with N = 0, the non-dimensional temperature Θ at x/D = 1 attains a relatively high value of 0.75. This behavior demonstrates a non-dimensional temperature jump from 0.5 to 0.75. For weak radiation with N = 0.01 the non-dimensional temperature Θ at x/D = 1 attains the value of $\Theta = 0.50$, that is the non-dimensional temperature of the right bounding surface. For limiting pure conduction with a high N = 10, the non-dimensional temperature distribution shows the negative sloped straight line ending with $\Theta = 0.5$ at x/D = 1.

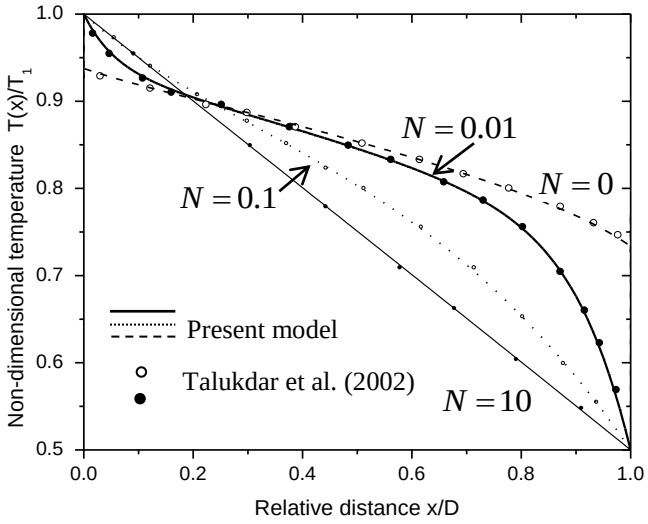

Fig.3 Non-dimensional temperature distributions for an absorbing-emitting gray material with optical thickness $\kappa_D = 1$ and surface emissivity $\varepsilon = 1$ for various conduction-radiation parameters N = 0. 0.01, 0.1 and 10.

For the limiting case of pure radiation with $N = 0$, the non-dimensional temperature distributions in gray materials with temperature ratio $T_1/T_2 = 0.5$, different surface emissivity and optical thickness, are plotted in Figure. 4. Notice that a different temperature ratio $T_2/T_1 = 0.5$ was used in Figure 3. To assess the goodness of the new strip model in describing the heat transfer phenomena for pure radiation with $N = 0$, the respective non-dimensionless temperature distributions are compared with those reported in the seminal work by Viskanta and Grosh (1962b). It is observable that for all optical thicknesses κ_D the results are of excellent quality. Specifically, the largest difference of about 2.6% corresponds to a high optical thickness $\kappa_D = 10$.

In Figure 4(a) for a small optical thickness K_D = 0.1 and surface emissivities ε = 0.1, 0.5 and 1, the non-dimensional temperatures in the gray material remain almost constant from the left to the right bounding surfaces.

In Figure 4(b) for a moderate optical thickness K_D = 1, the non-dimensional temperature curve remains constant for a surface emissivities ε = 0.1, and switches to monotonic sloped for higher surface emissivities of ε = 0.5 and 1. The curve slopes increase gradually with increments in the surface emissivity ε.

In Figure 4(c) for a large optical thickness K_D = 10, the non-dimensional temperature curves exhibit a parabolic behavior, which is accentuated with increments in the surface

emissivity going from ε = 0.1 to 1.

The non-dimensional heat flux is conveniently defined by the relation $\zeta = q/(\sigma T_{ref}^4)$, where q denotes heat flux. Non-dimensional heat fluxes computed by the present model for gray materials characterized with optical thickness $\kappa_D = 10$, temperature ratio $T_2/T_1 = 0.5$ and different values of the conduction-radiation parameter *N* are portrayed in Figure. 5. Here again, the surface emissivity takes two extreme values $\varepsilon = 1.0$ and $\varepsilon = 0.1$. In Figure 5, the conductive, radiative and total non-dimensional fluxes are represented by ζ_c, ζ_r and ζ_t, respectively. A variety of straight lines, concave lines and convex lines are observed in the figure. For the extreme case dealing with pure radiation (*N = 0*), the maximum number of iterations needed for convergence was 5. On the contrary, for dominant conduction (*N =10*), only 2 iterations were needed to achieve satisfactory convergence. Again, to maintain uniformity, a tolerance of 0.001 was pre-set in advance.

(a)

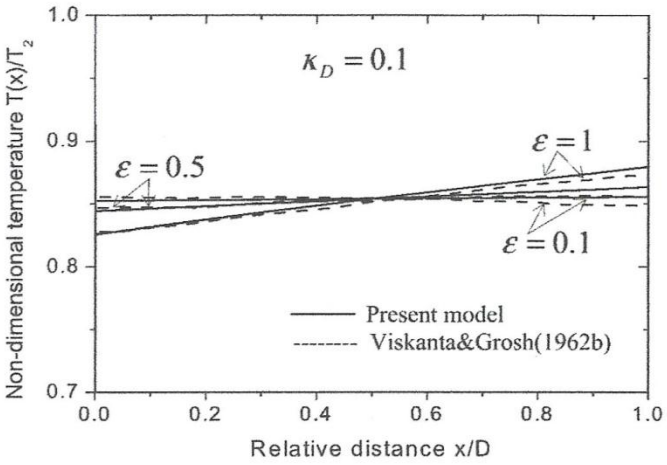
$\kappa_D = 0.1$
$\varepsilon = 0.5$
$\varepsilon = 1$
$\varepsilon = 0.1$
Present model
Viskanta&Grosh(1962b)
Non-dimensional temperature T(x)/T$_2$
Relative distance x/D
1.0
0.9
0.8
0.7
0.0
0.2
0.4
0.6
0.8
1.0

(b)

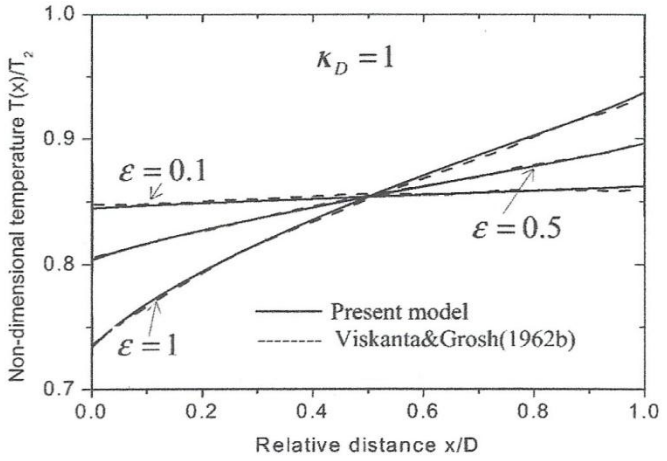
$\kappa_D = 1$
$\varepsilon = 0.1$
$\varepsilon = 0.5$
$\varepsilon = 1$
Present model
Viskanta&Grosh(1962b)
Non-dimensional temperature T(x)/T$_2$
Relative distance x/D
1.0
0.9
0.8
0.7
0.0
0.2
0.4
0.6
0.8
1.0

(c)

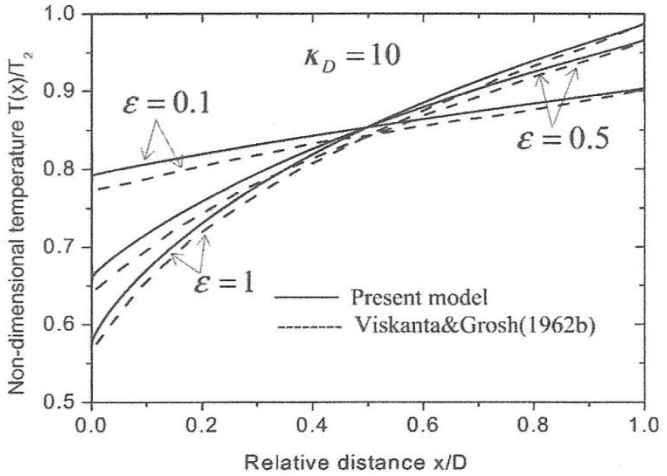
$\kappa_D = 10$
$\varepsilon = 0.1$
$\varepsilon = 0.5$
$\varepsilon = 1$
Present model
Viskanta&Grosh(1962b)
Non-dimensional temperature T(x)/T$_2$
Relative distance x/D
1.0
0.9
0.8
0.7
0.6
0.5
0.0
0.2
0.4
0.6
0.8
1.0

Fig. 4 Non-dimensional temperature distributions in an absorbing-emitting gray material for limiting pure radiation $N = 0$ and optical thicknesses $K_D = 0.1$, 1 and 10 combined with surface emissivities $\varepsilon = 0.1$, 0.5 and 1.

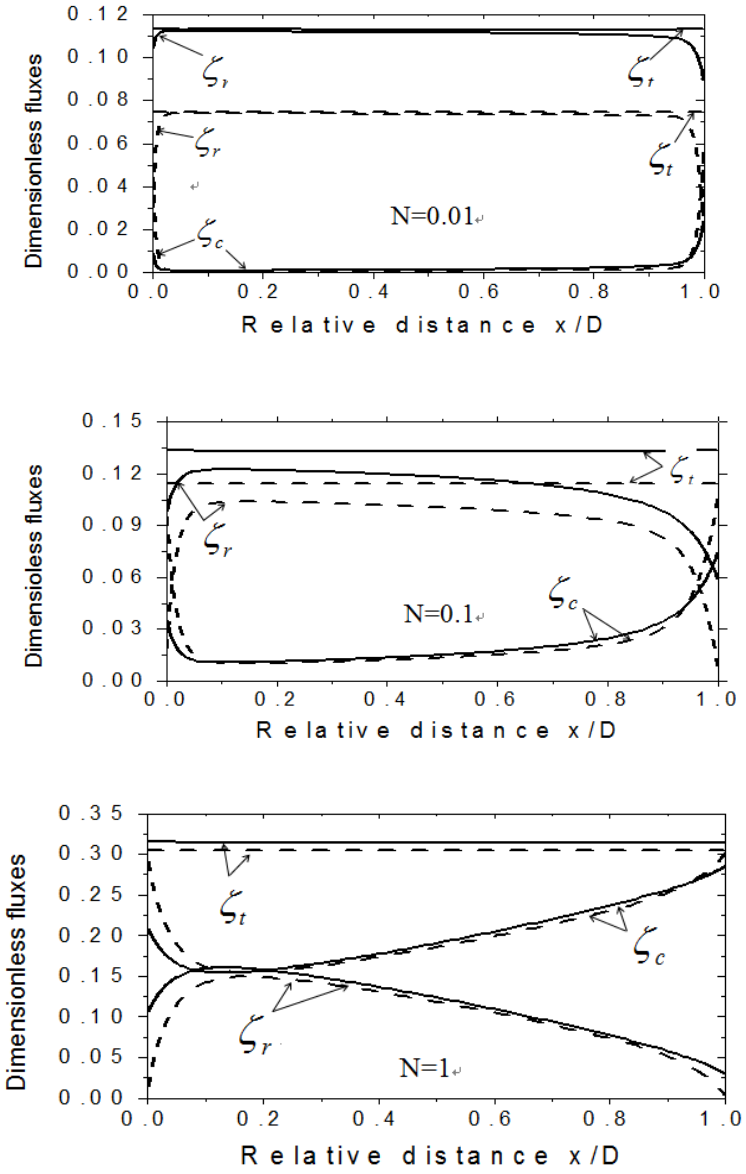

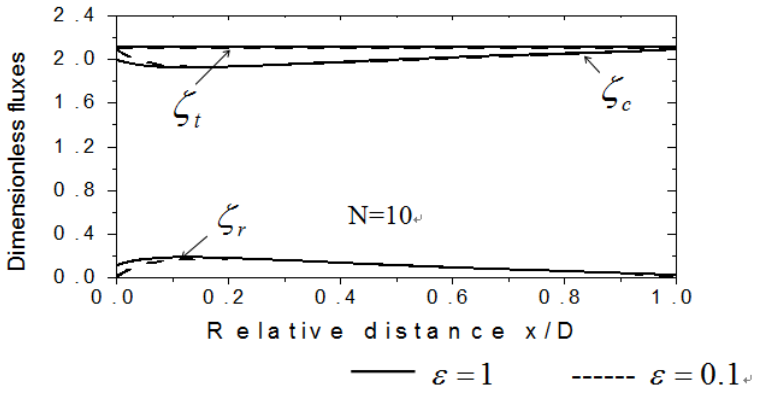

Fig.5 Non-dimensional total heat flux distributions for conduction-radiation parameters N = 0.1, 1 and 10 coupled with surface emissivities ε = 0.1 and 1.

The numerically-obtained non-dimensional total fluxes ζ_t are listed in Tables 1 and 2. It is observable that the numbers compared favorably with those reported in the seminal publication by Viskanta and Grosh (1962b).

Table 1 Non-dimensional total heat fluxes ζ_t for various optical thicknesses κ_D, temperature ratios T_1/T_2 and conduction-radiation parameters N under the influence of very high surface emissivities: $\varepsilon_1 = \varepsilon_2 = 1.0$.

κ_D	T_1/T_2	N	ζ_t	
			Present study	Viskanta and Grosh (1962b)
0.1	0.5	0	0.858	0.859
		0.01	1.079	1.074
		0.1	2.876	2.88
		1.0	20.846	20.88
		10	200.540	200.88
1.0	0.1	0	0.559	0.556
		0.01	0.631	0.658
		0.1	0.968	0.991
		1.0	4.192	4.218
		10.0	36.546	36.60
1.0	0.5	0	0.519	0.518
		0.01	0.567	0.596
		0.1	0.769	0.798
		1.0	2.570	2.60
		10.0	20.54	20.60

10.0	0.5	0	0.109	0.102
		0.01	0.113	0.114
		0.1	0.133	0.131
		1.0	0.315	0.315
		10.0	2.111	2.114

Table 2 Non-dimensional total heat fluxes ζ_t for various optical thicknesses κ_D, temperature ratios T_1/T_2 and conduction-radiation parameters N under the influence of very low surface emissivities: $\varepsilon_1 = \varepsilon_2 = 0.1$.

κ_D	T_1/T_2	N	ζ_t	
			Present study	Viskanta and Grosh (1962b)
0.1	0.5	0	0.0491	0.049
		0.01	0.277	0.267
		0.1	2.074	2.078
		1.0	20.044	20.08
		10.0	200.00	200.08
1.0	0.1	0	0.061	0.051
		0.01	0.198	0.22
		0.1	0.570	0.591
		1.0	3.809	3.752
		10.0	36.15	36.22
1.0	0.5	0	0.0476	0.047
		0.01	0.157	0.156
		0.1	0.402	0.393
		1.0	2.219	2.245
		10.0	20.19	20.25
10.0	0.5	0	0.036	0.036
		0.01	0.0874	0.090
		0.1	0.114	0.115
		1.0	0.304	0.297
		10.0	2.102	2.107

6. Conclusions

A new computational method, called the finite strip method is developed in this work dealing with the heat transfer analysis of simultaneous heat conduction and thermal radiation in

an absorbing and emitting gray material filling a planar slab. The finite strip method seeks to transform the integro partial differential equation of energy into a nonlinear system of algebraic equations. The computational efficiency of the finite strip method is verified through a series of critical tests utilizing gray materials accounting for a wide variety of thermal properties and optical properties, such as the conduction-radiation parameter N, the surface emissivity ε and the optical thickness κ_D.

Comparisons of the computed non-dimensional temperatures Θ and the non-dimensional heat fluxes ζ_t with their counterparts from reliable publications in the heat transfer literature demonstrate that the finite strip method is capable of delivering results of superb accuracy for engineering applications. Of equal importance, the finite strip method necessitates a lesser number of iterations, small CPU times and remarkable convergence when compared against the standard numerical methods, such as finite differences and finite elements. Surely, these are unique features attributed to the finite strip method.

Acknowledgements

The first author (SPCM) gratefully acknowledges the financial support provided by the Brazilian Federal Agency, CNPq.

References

Abramowitz, M. and Stegun, A. (editors) (1965), *Handbook of Mathematical Functions*, Dover, New York, NY.

Anteby, I., Shai, I. and Arbel A. (2000), Numerical calculations for combined conduction and radiation heat transfer in a semitransparent medium, *Numerical Heat Transfer, Part A: Fundamentals*, Vol. 37, pp. 359-371.

Arpaci, V. (1966), *Conduction Heat Transfer*, Addison–Wesley, Reading, MA.

Campo, A., Malpica, F. and Tremante, A. (1986), Contribution of thermal radiation to the temperature profiles of semi–transparent materials, *High Temperature–High Pressure*, Vol. 18, pp. 35-41.

Campo, A. and Tremante, A. (1987), Analysis of conduction–radiation heat transfer in planar media using a two–flux model, *Wärme–und Stoffübertragung* (Germany), Vol. 21, pp. 221–232.

Dai and Fang (2014), An approach to calculate transient heat flow through transparent materials, *American Journal of Heat and Mass Transfer*, Vol. 1, No. 1, pp. 30-37.

Howell, J. R., Siegel, R. and Mengüç, M. P., (2011), *Thermal Radiation Heat Transfer*, 5nd Edition, CRC Press, Boca Raton, FL.

Mishra, S. C. (1997), A novel computational approach for the solution of radiative heat transfer problems in participating media, PhD Thesis, Mechanical Engineering Department, Indian Institute of Technology, Kanpur, India.

Mishra, S. C., Talukdar, P., Trimis, D. and Durst, F. (2004) Effect of angular quadrature scheme on the computational efficiency of the discrete transfer method for solving radiative transport problem with participating medium, *Numerical Heat Transfer, Part B: Fundamentals*, Vol. 46, pp. 463-478.

Mishra, S. C., Roy, H. K. and Misra, N. (2006), Discrete ordinate method with a new and simple quadrature scheme", *Journal of Quantitative Spectroscopy & Radiative Transfer*, Vol. 101, pp. 249-262.

Mitalas, G. P. (1968), Calculation of transient heat flow through walls and roofs", *ASHRAE Transactions* Vol. 74, pp. 182-188.

Modest, M. F. (2013), *Radiative Heat Transfer*, 3nd Edition, Academic Press, Oxford, England, UK.

Press, W. H. et al. (1986), *Numerical Recipes*, Cambridge University Press, London, England, UK.

Ratzell III, A. C. and Howell, J. R. (1982), Heat transfer by conduction and radiation in one-dimensional planar medium using differential approximation, *ASME Journal of Heat Transfer*, Vol. 104, pp. 388-399.

Shah, N. G. (1979), New method of computational of radiation heat transfer combustion chambers, PhD Thesis, Mechanical Engineering Department, Imperial College, London, England, UK.

Talukdar, P. and Mishra, S. C. (2002), Analysis of conduction-radiation problem in absorbing, emitting and anisotropically scattering media using the collapsed dimension method, *International Journal of Heat and Mass Transfer*, Vol. 45, pp. 2159-2168.

Viskanta, R. and Grosh, R. J. (1962a), Heat transfer by simultaneous conduction and radiation in an absorbing medium, *ASME Journal of Heat Transfer*, Vol. 84, pp. 63-72.

Viskanta, R. and Grosh, R. J. (1962b), Effect of surface emissivity on heat transfer by simultaneous conduction and radiation, *International Journal of Heat and Mass Transfer*, Vol. 5, pp.729-734.

Viskanta, R. and Anderson, E. E. (1975), Heat transfer in semitransparent solids. In *Advances in Heat Transfer*, Irvine, T. E. and Hartnett, J. P. (editors), Vol. 11, pp. 317-441, Academic Press, Oxford, England, UK.